IR Spectra for Adsorbed CO on Various Alkali Metal Ion-Exchanged ZSM-5 Zeolites

Masahiro KATOH, Tatsuya YAMAZAKI,* and Sentaro OZAWA
Department of Biochemistry and Engineering, Faculty of Engineering, Tohoku University, Aramaki-Aoba, Aoba-ku, Sendai 980-77

(Received November 12, 1993)

Carbon monoxide adsorption on alkali metal ion-exchanged ZSM-5 zeolites was investigated by IR spectroscopy. The IR peak positions and intensities of adsorbed CO, and the change in the spectra with temperature are discussed. The IR spectra for physisorbed CO over ZSM-5 zeolites were assigned to the oriented species on a cation, such as M^+–C–O and M^+–O–C, and the loosely adsorbed CO in the ZSM-5 pore.

Zeolites are porous adsorbents consisting of SiO_4 and AlO_4 tetrahedra as a fundamental unit, and have exchangeable cations in the pore. The cation, the source of the electric field in a pore, can behave as an adsorption site for polar molecules, such as carbon monoxide. Zeolite adsorbents therefore generally exhibit high selectivity of adsorption for polar molecules. Although the adsorption of polar molecules on zeolites have been widely studied, most of them were concerned with the macro-characteristics of these adsorption systems, such as the relation between the selectivity and the hydrophilicity. Only recently were some studies reported concerning the microscopic behavior of polar adsorbates in zeolite pores. For example, Lercher et al. proposed models for clustered structure of H_2O[1] and H_2S[2] adsorbed on ZSM-5 zeolites using IR spectroscopy and thermogravimetry. Förster et al. performed a study in order to clarify CO adsorption on A-type zeolites, combining IR spectroscopy with a quantum chemical calculation and a vibration analysis.[3—5] Kustov et al.[6] characterized the adsorption sites for CO on ZSM-5 zeolites by IR spectroscopy combined with a quantum chemical calculation. Echoufi and Gelin[7] have reported on the formation of three types of physically adsorbed CO on a decationated Y zeolite. In addition, Bordiga et al.[8,9] carried out an IR investigation concerning CO adsorption on NaZSM-5, and also reported three modes of adsorbed CO species.

The present authors have been studying the adsorption of several non-polar gases on ZSM-5 zeolites by IR spectroscopy.[10—14] In these studies, it was found that a cation in the ZSM-5 zeolite pore strongly influences even a non-polar adsorbate, and that the characteristics of the adsorbed species on the cation site in the ZSM-5 zeolite pore can be simulated by a simple model. Thus, the results of work aimed at clarifying the characteristics of the physical adsorption of CO on a series of alkali metal ion-exchanged ZSM-5 zeolites using IR spectroscopy and adsorption potential calculation are presented in this paper.

Experimental

ZSM-5 adsorbents were prepared by a conventional ion-exchange method[10,11] from NaZSM-5 (SiO_2/Al_2O_3 = 23.3 : supplied by Tosoh Co., Ltd.). The ion exchanging rates were confirmed to be about 100% by atomic absorption spectroscopy or X-ray fluorescence spectroscopy. Silicalite (SiO_2/Al_2O_3=2120) was kindly provided by Professor Yashima, Tokyo Institute of Technology. The adsorbents were pretreated at 623 K in vacuo (7×10^{-3} Pa) for 8 h in an IR cell prior to IR measurements. CO gas purified by passing through a cold trap (at 77 K) was used as the adsorbate. The IR spectra were recorded on a JEOL JIR-100 FTIR spectrometer (resolution: 2 cm^{-1}, scan times: 200, TGS detector), mainly at 226 K, under several CO pressures ranging from 1.3 to 40 kPa. In addition, some measurements were carried out at several temperatures ranging from 178 to 299 K under a constant CO pressure of 3 or 6 kPa. The spectra of an adsorbed species were obtained by subtracting the spectrum of the gas-phase CO from the observed ones.

Results and Discussion

Adsorption Interaction and IR Peak Assignment. The IR spectra of adsorbed CO on ZSM-5 zeolites and a silicalite at 226 K are shown in Fig. 1. The IR band of the adsorbed species on silicalite was fairly broad, and had shoulders similar to the rotational wings of the gas phase CO (P- and R-branch). In addition, the peak position almost agreed with that of free CO (2143 cm^{-1}, indicated by the arrow in the figures).[15] These results suggest that the interaction of CO with the silicalite surface is weak, and, hence, the adsorbed CO retains some molecular rotational freedoms in the silicalite pore.

On the other hand, the IR absorption bands on the ZSM-5 zeolites comprised two or three peaks (Fig. 1 b—g). Two peaks (peaks I and II) appeared at the high-frequency side, and one peak (peak IV) appeared at the low-frequency side of the IR peak of gaseous CO. In addition, a peak (peak III) appeared around the position of free CO on HZSM-5 and LiZSM-5. All of these peaks (I, II, III, and IV) were assigned to those of physically adsorbed CO species for the following reasons: 1) The position of these peaks did not differ much from that of gaseous CO; 2) the intensities of these peaks reversibly varied with the CO pressure.

Peak III appeared only on HZSM-5 and LiZSM-5, and the peak position almost agreed with that in the silicalite-CO system. Therefore, this peak can be assigned to the physisorbed CO in ZSM-5 pore without the influence of electric field formed by a cation (silicalite like

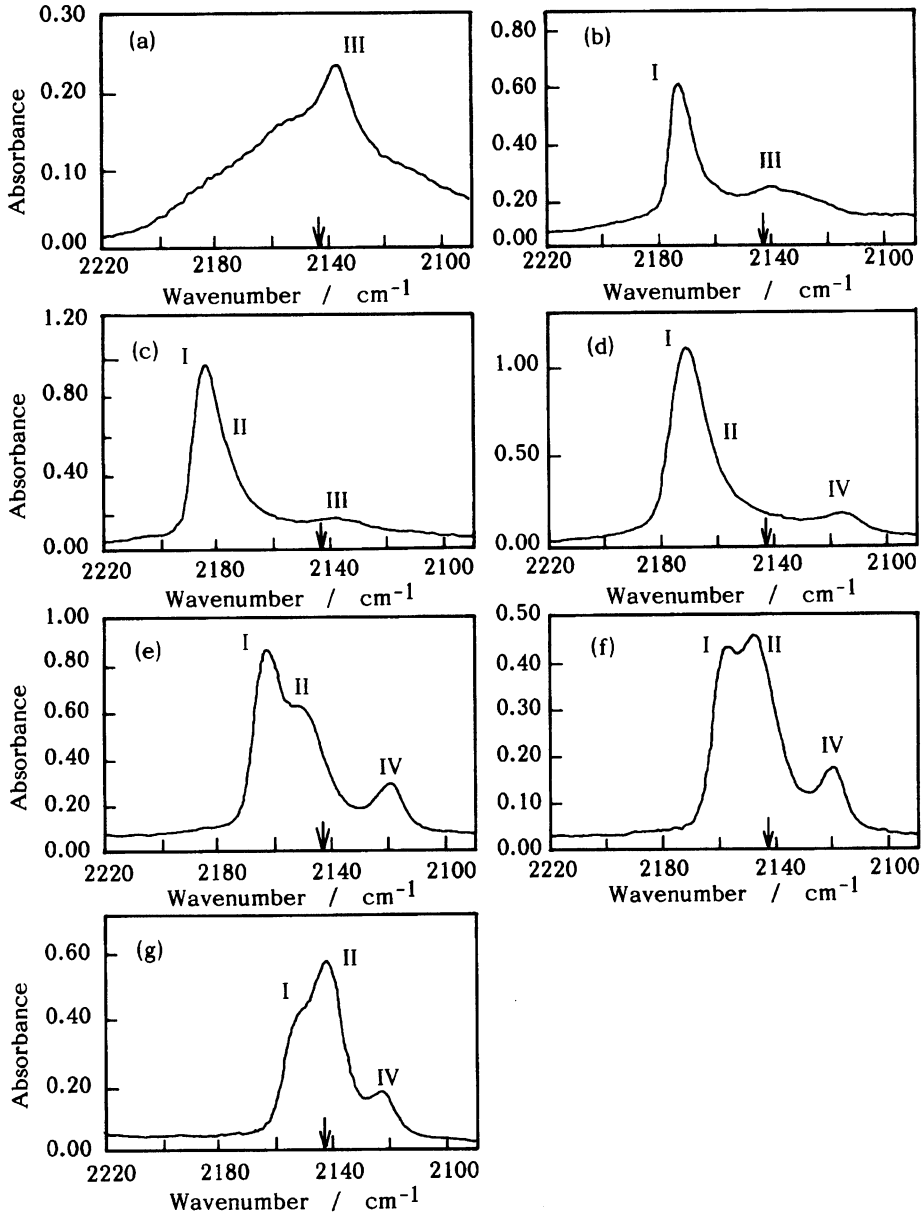

Fig. 1. Infrared spectra of adsorbed CO on silicalite and alkali metal ion-exchanged ZSM-5 zeolites at 226 K; (a) silicalite (13.2 kPa). (b) HZSM-5 (13.0 kPa). (c) LiZSM-5 (13.8 kPa). (d) NaZSM-5 (13.4 kPa). (e) KZSM-5 (13.0 kPa). (f) RbZSM-5 (13.4 kPa). (g) CsZSM-5 (14.1 kPa).

site). This consideration is coincident with the finding of Kustov et al., who assigned a peak appearing at 2140 cm^{-1} on HZSM-5 to physically adsorbed CO species.[6] It is reasonable that such sites exist in these zeolites, because small-size cations, such as H^+ or Li^+, can enter deeply into a pore wall consisting of a 5- or 6-membered oxygen ring,[10,11] and the pore wall largely shields the electric field created by the cation.

Bordiga et al.[8,9] reported on the appearance of an IR absorption band ascribed to physisorbed CO retaining some rotational freedom in the NaZSM-5 pore at 77 K. However, this was not the case in the present study. This discrepancy might have been caused by the difference in the adsorption temperature and the cation (Na^+) content in ZSM-5. Namely, the adsorbates may have been distributed to the cationic adsorption site in preference to the silicalite-like site, because the amount of adsorption is smaller, and the content of the cation was higher in the present study.

In the cases of HZSM-5 and LiZSM-5, the intensity ratios of peak III to peak I or peak II increased with an increase in the CO pressure. This means that the amount of adsorbed species giving rise to peak III increased more rapidly with the CO pressure than did those of peak I and peak II in these zeolites. In contrast, peak III was not observed in ZSM-5 zeolites ion-exchanged with an alkali metal cation other than Li^+, showing that the silicalite-like site (without electric field) did

not play any important role. Thus, the cation sites are predominant in these zeolites.

The positions of peak I, peak II, and peak IV are plotted as a function of the size of the cation exchanged in the zeolites in Fig. 2. This figure shows that both peak I and peak II in high-frequency side gradually shifted to a lower frequency with an increase in the size of the cation exchanged, whereas peak IV on the low-frequency side shifted toward a higher frequency. In other words, all of the IR peaks gradually approached the position of free CO as the size of the ion in the zeolite increased. Since the strength of the electric field formed by a cation is expected to be inversely proportional to the distance between the cation and the adsorbate, the correlation given in Fig. 2 seems to be reasonable; a ZSM-5 zeolite having a smaller cation is able to interact more strongly with CO and, hence, to greatly shift the peaks.

The IR peak shift ($\Delta\omega$) of adsorbed CO due to the cations was evaluated based on the adsorption model, as shown in Fig. 3. This model is an extension of one proposed for non-polar adsorbates,[12—14] and includes an interaction between the permanent dipole moment of the adsorbate molecule and the electric field in the adsorbent pore. Since the details concerning the original model were given elsewhere,[12—14] only a brief description is presented here. Namely, the $\Delta\omega$ value was calculated using the following equation:[16]

$$\Delta\omega = B_e/(hc\omega_e)(U'' - 3aU'), \tag{1}$$

where U', U'', B_e, h, c, ω_e, and a are the first and second derivatives of the adsorption potential (U) with respect to the reduced coordinate, the rotational constant, Planck's constant, the velocity of light, the frequency of the harmonic oscillation, and the anharmonicity constant of the third term in the potential of

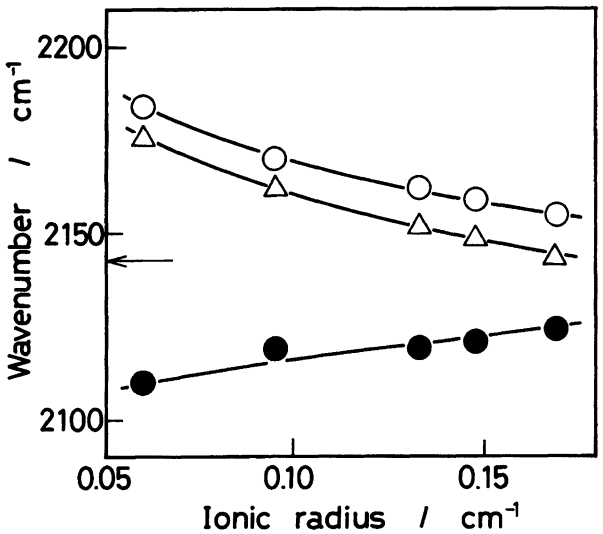

Fig. 2. Correlation between the ionic radius of cation and the peak positions; ○: peak-I, △: peak-II. ●: peak-IV.

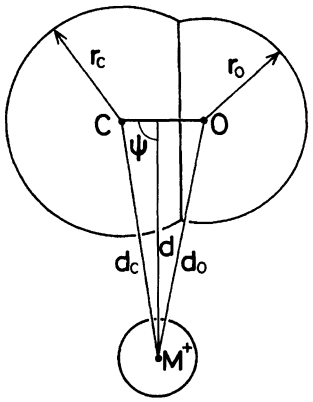

Fig. 3. Interaction model between isolated cation and CO molecule. r_C: van der Waals radius of carbon, r_O: van der Waals radius of oxygen. ψ: orientation angle, d: distance between center of CO molecule and cation. d_C: distance between carbon and cation. d_O: distance between oxygen and cation.

a free molecule, respectively. In general, since the absolute value of U'' is smaller than that of U', Eq. 1 can be approximated by Eq. 2.

$$\Delta\omega = -3aU'B_e/(hc\omega_e). \tag{2}$$

The potential energy, (U), was calculated by the following equations:

$$U_D = A_C/d_C{}^6 + A_O/d_O{}^6, \tag{3}$$

$$U_R = B_C/d_C{}^{12} + B_O/d_O{}^{12}, \tag{4}$$

$$U_P = -q^2\{\alpha_M + \gamma/3(3\cos^2\psi - 1)\}/2d^4, \tag{5}$$

$$U_Q = qQ(3\cos^2\psi - 1)/2d^3, \tag{6}$$

$$U_M = -q\mu\cos\psi/d^2, \tag{7}$$

and

$$U = U_D + U_R + U_P + U_Q + U_M, \tag{8}$$

where U_D, U_R, U_P, U_Q, U_M, A_i, B_i, q, α_M, γ, and μ, are the potential energies originating from the dispersion force, the repulsion force, the induced dipole interaction, the quadrupole interaction, the dipole interaction, the dispersion constant, the repulsion constant (subscript i represents an atom in CO concerned), the electric charge of the cation, the mean of the molecular polarizability, the anisotropy of the molecular polarizability, and the dipole moment of the CO molecule,

Table 1. Characteristic Properties of Atoms in CO Molecule[a]

Atom	Atomic radius, r_j	Polarizability α_j	Diamagnetic susceptibility, x_j
	nm	10^{-24}cm^3	10^{-29}cm^{3}molec^{-1}
C	0.17[19]	2.13 [20]	−1.52[20]
O	0.15[19]	0.831[20]	−1.16[20]

a) Values were taken from reference indicated in square brackets.

Table 2. Values of Physical Quantities Used in the Potential Calculation[a)]

Cation	Ionic radius, r_i	Polarizability α_i	Diamagnetic susceptibility, x_i	Dispersion constant[b)] A_C	A_O	Repulsive constant[c)] B_C	B_O
	nm	10^{-24}cm^3	10^{-29}cm^{3}molec^{-1}	10^{-42}J mol^{-1}cm^6		10^{-87}J mol^{-1}cm^{12}	
Li^+	0.060[21]	0.029 [22]	−0.105 [22]	−0.109	−0.0717	0.395	0.0759
Na^+	0.095[21]	0.19 [22]	−0.70 [22]	−0.717	−0.473	1.32	0.301
K^+	0.133[21]	0.84 [22]	−2.77 [22]	−3.11	−2.02	4.71	1.31
Rb^+	0.148[21]	1.41 [22]	−5.80 [22]	−5.40	−3.61	7.96	2.46
Cs^+	0.169[21]	2.44 [22]	−9.10 [22]	−9.21	−6.08	15.6	5.27

a) Values were taken from reference indicated in square brackets. b) Calculated by the equation $A_j=6mc^2\cdot\alpha_i\alpha_j(\alpha_i/x_i+\alpha_j/x_j)$. c) Calculated by the equation $B_j=-0.5A_j(r_i+r_j)^6[1-(1/3A_j)\alpha_j q^2(r_i+r_j)^2]$.

Table 3. Characteristic Properties of CO[a)]

R[b)]	α_M[c)]	γ[d)]	Q[e)]	μ[f)]	ω_e[g)]	B_e[h)]	a[i)]
nm	10^{-24}cm^3	10^{-24}cm^3	10^{-26}esu cm^2	10^{-18}esu cm	cm^{-1}	cm^{-1}	
0.1128[23]	1.94[24]	0.541[24]	−1.94[25]	0.112[26]	2169.8[23]	1.931[23]	−2.70[23]

a) Values were taken from reference indicated in square brackets. b) Atomic distance. c) Mean polarizability. d) Polarizability. e) Quadrupole moment. f) Dipole moment. g) Harmonic oscillator. h) Rotational constant. i) Anharmonicity constant.

respectively. In addition, d, d_C, d_O, and ψ are the distances and the orientation angle, as defined as in Fig. 3. The calculation was carried out using physical parameters of free CO (Tables 1, 2, 3, and 4) as those of the adsorbed CO as an approximation. The interaction of CO with the zeolite pore wall was disregarded in the calculation, since the peak position of the CO adsorbed on silicalite was nearly equal to that of free CO, indicating little effect of the pore wall interaction on $\Delta\omega$.

The resultant interaction potential energies and IR peak positions are shown as a function of the orientation angle (ψ) in Figs. 4a and 4b, respectively. As can be seen in Fig. 4a, two minima appear in the potential curve irrespective of the kind of adsorbent; it is attributed to the quadrupole interaction, which is strongly attractive at ψ-values of 0° and 180°. From now on, we refer to the structures of the adsorbed species with a ψ of 0° and 180° as structure A (M^+–CO species) and structure B (M^+–OC species), respectively. Structure A is evaluated to be more stable than structure B by about 1.5 kJ mol^{-1} base on the difference in the dipole-electric field interaction. These small differences in the potential energies between two minima permit two types of adsorbed species to exist at the same time in the zeolite pore, except at a very low temperature.

Table 4. First Derivatives of α, γ, Q, and μ with Respect to the Bond Length[a)]

$d\alpha_M/dR$	$d\gamma/dR$	dQ/dR	$d\mu/dR$
10^{-16}cm^2	10^{-16}cm^2	10^{-18}esu cm	10^{-10}esu
1.53[27]	2.38[27]	2.37[28]	−3.13[27]

a) Values were taken from reference indicated in square brackets.

On the other hand, the direction of the IR peak shift for adsorbed CO on the cation were found to drastically change depending upon the orientation angle, as can be seen in Fig. 4b. Namely, structure A gave rise to a high-frequency shift, while structure B gave rise to a low-frequency shift. In addition, a smaller cation resulted in a larger peak shift. These tendencies were parallel with the experimental observations. Consequently, peak I observed in the present study can be assigned to a species with a small ψ value, like structure A (A-1 species), while peak IV can be assigned to a species with a larger ψ value, like structure B. In addition, peak II may also be assigned to a structure A type species (A-2 species) on the basis of the peak position and cation size dependency.

The appearance of two components for a structure A type species would be attributed to two kinds of distinguishable cation sites in the ZSM-5 pore. Two kinds of cation sites for NaZSM-5,[17] resulting from the straight and the sinusoidal channels of the ZSM-5 zeolite, were recently suggested by Ohgushi and Kataoka. Although details concerning the nature and positions of these adsorption sites in the zeolite are not clear at the present stage, it can be said based on the peak position that the orientation of the A-1 species giving rise to peak I would be more upright on the cationic adsorption site than those of the A-2 species.

The intensity ratio of peak I to peak II increased with an increase in the amount of adsorption. Namely, peak II was firstly developed in the region of a small amount of adsorption, and peak I subsequently increased at higher coverage. If the A-1 and A-2 species are formed on two kinds of respective sites, the results mentioned above imply that the A-2 species (peak II) involves

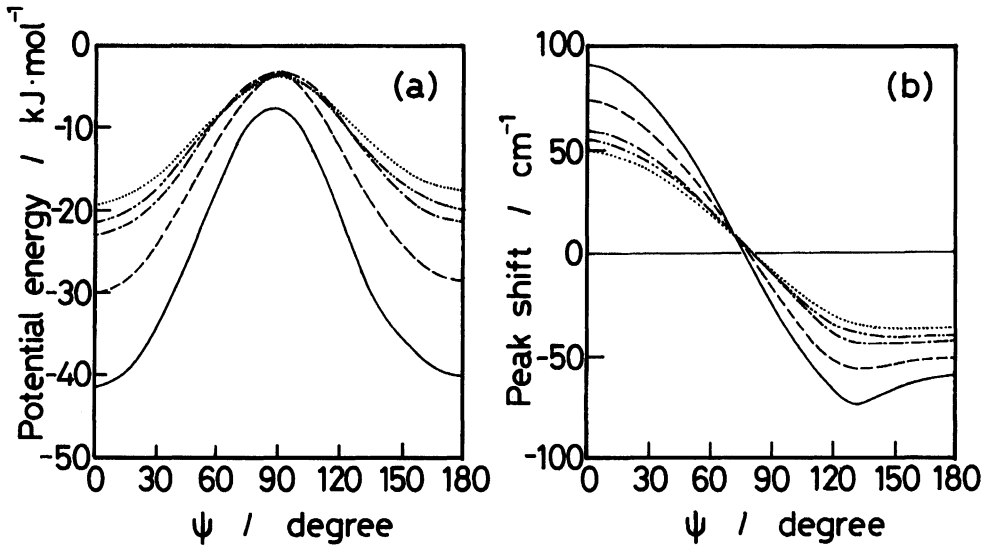

Fig. 4. Interaction potentials (a) and theoretical IR peak shifts (b) of adsorbed CO as a function of molecular orientation angle; —: LiZSM-5, - - -: NaZSM-5, –·–: KZSM-5, –··–: RbZSM-5, ····: CsZSM-5.

a stronger interaction with the site than that in A-1 species (peak I).

An alternative explanation for the appearance of the doublet peaks (I and II) could be that a difference in the interaction between the adsorbed CO molecules shifted the CO stretching band in a different way. Bordiga et al. recently found two peaks at the high-frequency side with respect to the IR position of free CO in a NaZSM-5 – CO system. They assigned the higher frequency peak (2178 cm^{-1}) to a strongly interacting Na^+–CO species, while the other one (2170 cm^{-1}) was assigned to a species being coordinated by more than one CO molecule, $Na^+(CO)_n$.[8] However, the intensity of peak I, the higher frequency peak in this work (ca. 2170 cm^{-1}), relative to peak II (ca. 2162 cm^{-1}) increased with an increase in the amount of adsorption. Therefore, peak II should probably be assigned to a strongly adsorbing species; it can not be assigned to a multi-coordinated CO species.

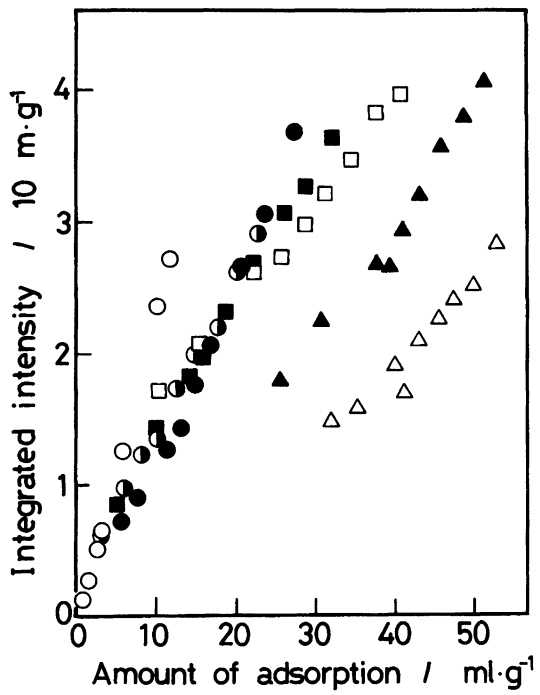

Fig. 5. Integrated IR band intensities of adsorbed CO on silicalite and ZSM-5 zeolites as a function of amount of CO adsorption; ○: silicalite. ●: HZSM-5, △: LiZSM-5, ▲: NaZSM-5, □: KZSM-5, ■: RbZSM-5, ◑: CsZSM-5.

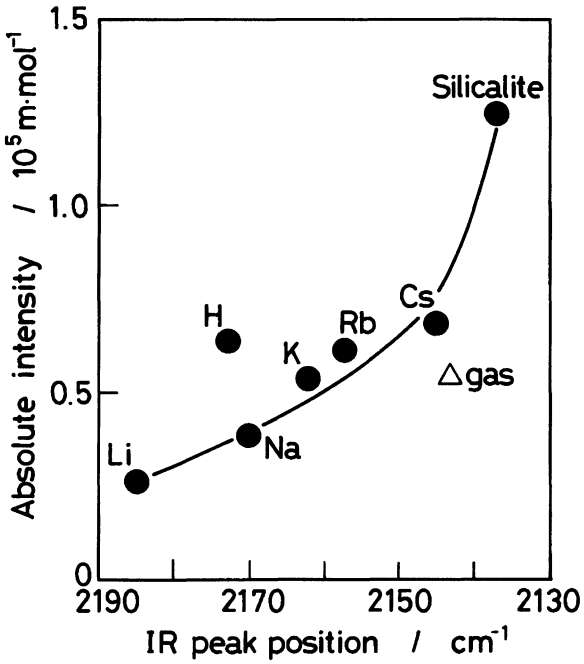

Fig. 6. Correlation between the integrated IR band intensities per an adsorbed CO (absolute intensity) and the peak position of main peak.

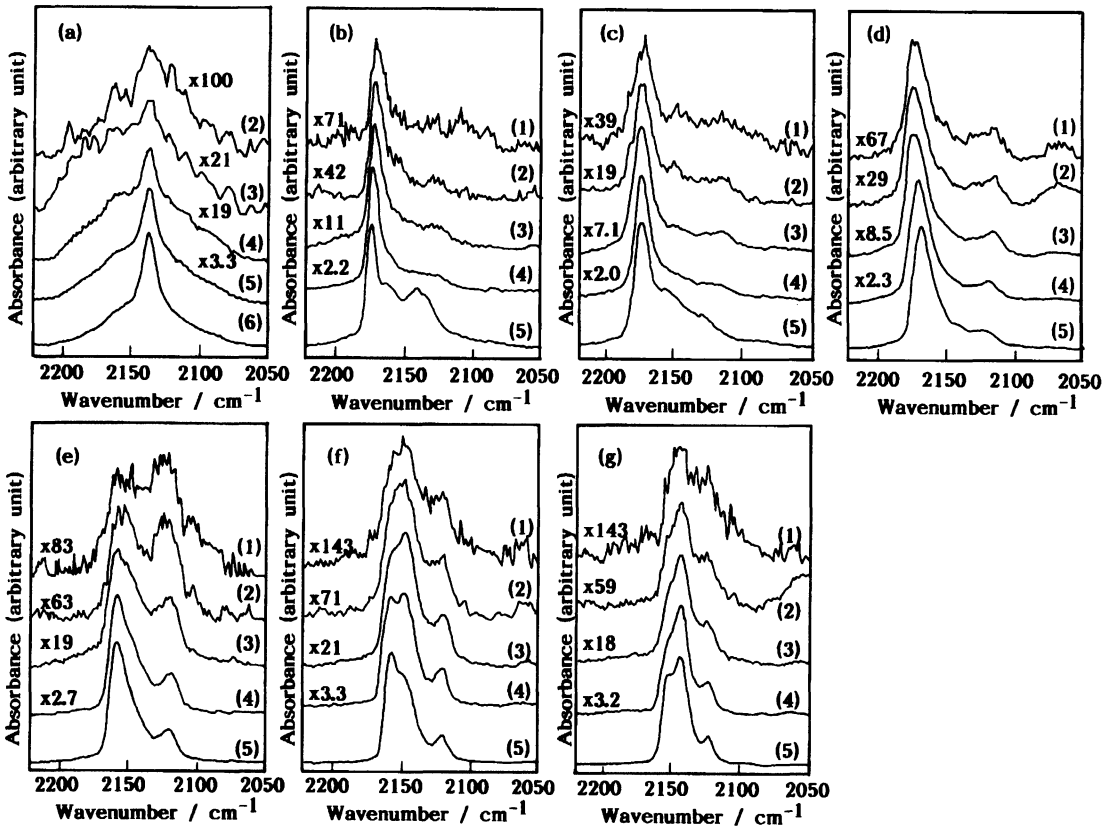

Fig. 7. Normalized infrared spectra of adsorbed CO on silicalite and ZSM-5 zeolites at several adsorption temperatures; (a): silicalite (6 kPa), (b): HZSM-5 (3 kPa), (c): LiZSM-5 (3 kPa), (d): NaZSM-5 (3 kPa), (e): KZSM-5 (3 kPa), (f): RbZSM-5 (3 kPa), (g): CsZSM-5 (3 kPa); (1) at room temperature (294—299 K), (2) at 273 K, (3) at 257 K, (4) at 226 K, (5) at 199 K, (6) at 178 K.

In contrast to the appearance of two peaks for the structure A species, only one peak was observed for structure B over all of the ZSM-5 zeolites studied. This result seems to be reasonable, since the magnitude of peak shift at the low-frequency side was estimated to be almost constant over a wide range of orientation angles, i. e. from 120° to 180°, as shown in Fig. 4b. Therefore, even if there were two structure B species, they probably could not be distinguished.

IR Band Intensity of Adsorbed Species. The IR integrated intensities (S) of the adsorbed CO are plotted in Fig. 5 as a function of the amount of adsorption. The peak area was integrated in the region between 2080 and 2220 cm^{-1}. In the case of silicalite, the intensity increased linearly with the amount of adsorption. Therefore, the intensity per one admolecule (absolute intensity; which was defined by $1/nl\int_\nu \ln(I_0/I)\mathrm{d}\nu$, where n, l, I_0, I, and ν are the number of moles of the vibrator in unit volume, the thickness of the sample, the intensity of incident light, the intensity of transmitted light, and the wavenumber, respectively.) was estimated by a least-square method to be 12×10^4 m mol^{-1}, which corresponded to almost twice that of free CO.[18] The enhancement of the IR intensity due to adsorption has frequently been reported in the literature. Although the details concerning the mechanism are not clear, it can at least be said that the enhancement was caused by a surface force of the silicalite wall. Seanor and Amberg reported on the correlation between the IR intensity and the IR peak position of adsorbed CO.[18] According to their study, the intensity was enhanced when the peak position of the adsorbed CO shifted to a low frequency with respect to that of free CO. In the present study, the IR peak position of CO adsorbed on silicalite was 2137 cm^{-1}, which was 6 cm^{-1} lower than that of the free CO (2143 cm^{-1}). The enhanced intensity was, therefore, present on the line described by Seanor and Amberg.[18]

On the other hand, an analysis of the IR intensity (S) of adsorbed CO on ion-exchanged ZSM-5 zeolites encountered some difficulty because their bands consisted of several peaks. However, taking the point that the major part of the S-value was contributed from the peak of structure A into account, the relation between the band intensity and the position of the main peak could be discussed as follows. The integrated IR intensities per one adsorbed CO molecule (absolute intensities) were evaluated in a similar manner with that in silicalite, and are plotted in Fig. 6 as a function of the peak position. These plots are similar to the correla-

tion expected by Seanor and Amberg. The estimated absolute intensities are $2—7\times10^4$ m mol^{-1}; the values increased with an increase in the size of the exchanged cation (Fig. 6). Namely, the stronger was the interaction between CO and a cation, the weaker was the IR intensity of the adsorbed CO. Since the IR intensity is proportional to the square of $(d\mu/dR)$, the results mentioned above seem to suggest that the strong field of the cation suppressed any change in the dipole moment of the CO molecule in C–O stretching vibration, but that a surface force of the zeolite pore enhanced it.

The plot for the HZSM-5 is located at rather an irregular position in Fig. 6. Several explanations might be possible for this system, including a very small cation; however, a detailed analysis is left to the future.

Variation of IR Spectra with Adsorption Temperature. The IR spectra for CO adsorbed on several alkali metal ion-exchanged ZSM-5 at various temperature, normalized with respect to peak height, are shown in Fig. 7. The spectra at the highest temperature was firstly obtained, followed by those at lower temperatures at a constant pressure (indicated in the caption). As the adsorption temperature increased, the degree of splitting between peaks I and II decreased, and peak II could not be distinguished above 0 °C. In addition, both sides of the main peaks (peak I) in the spectra rose slightly as the temperature increased, especially in the case of silicalite. This rise may be attributed to a restoring of the rotational freedom for an admolecule, because the shape of the spectra was similar to that of the rotational wings of free CO. These facts indicated that the motional freedom of adsorbed CO was widely changed in the temperature range studied.

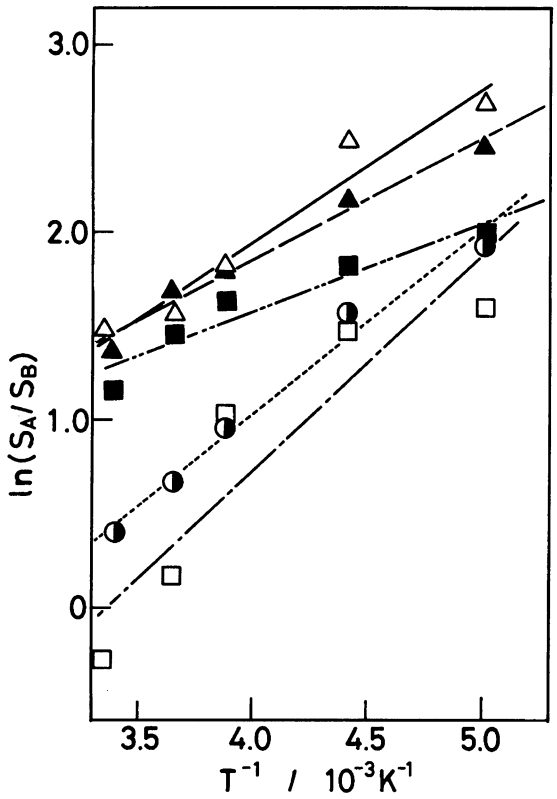

Fig. 8. Plots of $\ln(S_A/S_B)$ as a function of $1/T$, where S_A and S_B are integrated intensities of structure A and structure B, and fitted lines; —△—: LiZSM-5, - - -▲- - -: NaZSM-5, – · –□– · –: KZSM-5, – · · –■– · · –: RbZSM-5, · · · ·◑· · · ·: CsZSM-5.

It should also be noted that the peak area ratio of structure-A to structure-B (S_A/S_B) decreased with an increase in the adsorption temperature. If S_A and S_B are far below saturation, the difference in the adsorption potential energies between structure-A and structure-B can be estimated from the temperature dependence of (S_A/S_B). Hence, the logarithms of (S_A/S_B) are plotted as a function of $1/T$ in Fig. 8. Although there is considerable scattering, the result shows that the structure-A is more stable than structure-B by 4—10 kJ mol^{-1} in ZSM-5.

Conclusion

The IR spectra for adsorbed CO were studied over several alkali metal ion-exchanged ZSM-5 zeolites. The spectra of CO physisorbed on zeolites at 226 K consisted of 2 or 3 peaks; they were assigned to oriented species on a cation, such as M^+–C–O and M^+–O–C, and a loosely adsorbed CO in zeolite pores. Two IR peaks (peak I and peak II) being assigned to the M^+–C–O species appeared on the high-frequency side, while an IR peak (peak IV) for the M^+–O–C species appeared on the low-frequency side with respect to gaseous CO. The magnitude of the IR peak shift decreased with an increase in the size of an exchanged cation, because of the decrease in the strength of the electric field on the cation. On the other hand, the IR peak intensities for adsorbed CO was enhanced to twice that of free CO on silicalite which does not have any cation, although the intensities of IR peaks on ZSM-5 zeolites were reduced by the effects of the exchanged cation.

References

1) A. Jentys, G. Warecka, M. Derewinski, and J. A. Lercher, *J. Phys. Chem.*, **93**, 4837 (1989).
2) C. L. Garcia and J. A. Lercher, *J. Phys. Chem.*, **96**, 2230 (1992).
3) M. Grodzicki, H. Förster, R. Piffer, and O. Zakharieva-Pencheva, *Catal. Today*, **3**, 75 (1988).
4) H. Böse, H. Förster, W. Frede, and M. Schumann, "Proc. 6th Int. Zeolite Conf., Reno, 1983," ed by D. Olsen and A. Bisio, Butterworths, Guildford (1984). p. 201.
5) H. Böse and H. Förster, *J. Mol. Struct.*, **218**, 393 (1990).
6) L. M. Kustov, V. B. Kazansky, S. Beran, L. Kubelková, and P. Jirù, *J. Phys. Chem.*, **91**, 5247 (1987).
7) N. Echoufi and P. Gelin, *J. Chem. Soc., Faraday Trans.*, **88**, 1067 (1992).
8) S. Bordiga, E. E. Platero, C. O. Arean, C. Lamberti,

and A. Zecchina, *J. Catal.*, **137**, 179 (1992).
9) S. Bordiga, D. Scarano, G. Spoto, and A. Zecchina, *Vib. Spectrosc.*, **5**, 69 (1993).
10) T. Yamazaki, I. Watanuki, S. Ozawa, and Y. Ogino, *Langmuir*, **4**, 433 (1988).
11) T. Yamazaki, I. Watanuki, S. Ozawa, and Y. Ogino, *Bull, Chem. Soc. Jpn.*, **61**, 1039 (1988).
12) T. Yamazaki, S. Ozawa, and Y. Ogino, *Mol. Phys.*, **69**, 369 (1990).
13) T. Yamazaki, I. Watanuki, S. Ozawa, and Y. Ogino, *Mol. Phys.*, **73**, 649 (1991).
14) T. Yamazaki, M. Katoh, S. Ozawa, and Y. Ogino, *Mol. Phys.*, **80**, 313 (1993).
15) G. Hertzberg, "Spectra of Diatomic Molecules," 2nd ed, Van Nostrand, New York (1950), p. 62.
16) A. D. Buckingham, *Trans. Faraday Soc.*, **56**, 753 (1960).
17) T. Ohgushi and S. Kataoka, *J. Colloid Interface Sci.*, **148**, 148 (1992).
18) D. A. Seanor and C. H. Amberg, *J. Chem. Phys.*, **42**, 2967 (1965).
19) A. Bondi, *J. Phys. Chem.*, **68**, 441 (1964).
20) J. O. Hirschfelder, C. F. Curtis, and R. B. Bird, "Molecular Theory of Gas and Liquids," Wiley, London (1954), p. 942.
21) L. Pauling, "The Nature of the Chemical Bond," 3rd ed, Cornell University Press, Ithaca (1966), p. 518.
22) R. M. Barr and G. C. Bratt, *J. Phys. Chem. Solid*, **12**, 154 (1960).
23) K. P. Huber and G. Hertzberg, "Molecular Spectra and Molecular Structure IV," Van Nostrand, New York (1979), p. 166.
24) R. D. Amos, *Chem. Phys. Lett.*, **70**, 613 (1980).
25) W. L. Meerts, F. H. de Leeuw, and A. Dymanus, *Chem. Phys.*, **22**, 319 (1977).
26) C. A. Burros, *J. Chem. Phys.*, **28**, 427 (1958).
27) K. K. Sunil and K. D. Jordan, *Chem. Phys. Lett.*, **145**, 377 (1988).
28) R. D. Amos, *Chem. Phys. Lett.*, **68**, 536 (1979).